Short Communication

Discerning the inefficacy of hydroxyl radicals during perfluorooctanoic acid degradation

Hassan Javed [a, b], Cong Lyu [c], Ruonan Sun [d], Danning Zhang [a, d], Pedro J.J. Alvarez [a, b, d, *]

[a] NSF Engineering Research Center for Nanotechnology Enabled Water Treatment (NEWT), USA
[b] Dept. of Chemistry, Rice University, Houston, TX, 77005, USA
[c] Key Lab of Groundwater Resources and Environment, Jilin University, Changchun, PR China
[d] Dept. of Civil and Environmental Engineering, Rice University, Houston, TX, 77005, USA

HIGHLIGHTS

- Resolved ambiguity about the role of hydroxyl radicals in PFOA degradation by AOPs.
- Compared PFOA degradation by UV photolytic versus UV + H_2O_2 treatment systems.
- H_2O_2 may counterproductively consume UV irradiation and hinder PFOA photolysis.
- Hydroxyl radicals do not enhance or provide ancillary benefits to PFOA degradation.

GRAPHICAL ABSTRACT
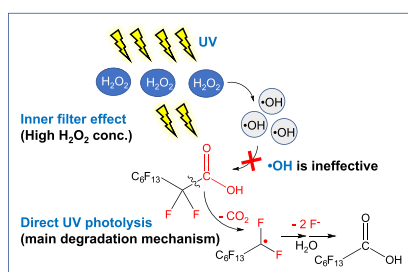
ABSTRACT

Perfluorooctanoic acid (PFOA) is a recalcitrant contaminant of emerging concern, and there is growing interest in advanced oxidation processes to degrade it. However, there is ambiguity in the literature about the efficacy of hydroxyl radicals (•OH) for degrading PFOA. Here, we resolve this controversy by comparing PFOA degradation by UV photolysis (254 nm, 6×10^{-6} E/L.s) versus UV + H_2O_2, which produces •OH. We optimized •OH production in a UV + H_2O_2 system using nitrobenzene (NB) as a •OH probe, but even under optimized conditions (i.e., 5 g/L H_2O_2), no significant difference occurred in PFOA removal by UV photolysis (21.1 ± 0.4%) versus UV + H_2O_2 (19.7 ± 0.7%) after 1-day treatment. Both treatments also resulted in similar daughter by-product concentrations and defluorination efficiencies (9.5 ± 1.7% for UV photolysis and 6.8 ± 1.0% for UV + H_2O_2), which indicates that •OH is ineffective towards PFOA degradation and infers that other degradation mechanisms that are independent of •OH production should be explored.

1. Introduction

Perfluoroalkyl substances (PFASs) are a class of over 3000 industrial chemicals that are contaminants of emerging concern due to their potential for bioaccumulation and persistence (Gómez et al., 2011; Saleh et al., 2019; Suja et al., 2009). PFOA is a widely researched PFAS that was historically used in leather, paper packaging, aqueous film forming foams (AFFFs) and as an additive to aviation fluid (Lopes da Silva et al., 2017). PFOA can also be formed in the environment through natural degradation of perfluorinated

---

precursors such as 8:2 fluorotelomer alcohols (Ellis et al., 2004; Ju et al., 2008; Vestergren et al., 2008). However, PFOA is relatively recalcitrant due to its abundant high-strength C–F bonds (116 kcal/mol) (Lin et al., 2012; Liou et al., 2010).

Several advanced oxidation and advanced reduction processes have been shown to degrade PFOA, including UV-Fenton (Tang et al., 2012), UV-Fe(III) (Liu et al., 2013), sonochemical (Cheng et al., 2008; Lin et al., 2015; Vecitis et al., 2008), catalyzed H_2O_2 propagation (CHP) reactions (Mitchell et al., 2014), electrochemical (Gomez-Ruiz et al., 2017; Le et al., 2019; Schaefer et al., 2017; Urtiaga et al., 2015; Zhuo et al., 2011), UV, peroxone and heat-activated $S_2O_8^{2-}$ (Eberle et al., 2017; Hori et al., 2005; Liu et al., 2012; Zhang et al., 2019), UV-SO_3^{2-} (Song et al., 2013), and reduction with solvated electrons (Park et al., 2009) and nano-scale zerovalent iron (NZVI) (Arvaniti et al., 2015; Hori et al., 2006). Some studies indicate that •OH may have an ancillary role in PFOA degradation. For example, tert-butyl alcohol (a •OH scavenger) decreased the PFOA defluorination efficiency in a UV-Fenton treatment system (Tang et al., 2012). Similarly, we observed that other •OH scavengers hinder PFOA defluorination in the presence of UV and Fe(III) (Liu et al., 2013). In these systems, •OH was proposed to enhance PFOA degradation by either initiating PFOA decarboxylation (pathway 3, Figure S1) or by accelerating the conversion of intermediate perfluorinated organic radical to perfluorinated alcohol (pathway 4, Figure S1). Several other groups have also shown that •OH may assist PFOA degradation (Chen et al., 2016, 2015; 2011; Gomez-Ruiz et al., 2018; Huang et al., 2016b; Lin et al., 2012; Song et al., 2012). However, other studies indicate that •OH is ineffective in degrading PFOA (Hori et al., 2004; Szajdzinska-Pietek and Gebicki, 2000).

This paper seeks to clarify ambiguity in the literature about the role of •OH in PFOA degradation. UV + H_2O_2 is a well-known advanced oxidation process (AOP) that relies primarily on •OH generation (Khan et al., 2018; Xu et al., 2009). We gain insights into the role of •OH in PFOA degradation by comparing UV photolytic treatment versus UV + H_2O_2, using nitrobenzene (NB) as •OH probe to optimize H_2O_2 concentrations. Furthermore, we report electrical energy per order (EE/O) for our reactions to facilitate energy requirement comparisons with other studies.

2. Materials and methods

2.1. Materials

Perfluorooctanoic acid (95% purity), perfluoroheptanoic acid (99% purity), perfluorohexanoic acid (≥97% purity), perfluoropentanoic acid (97% purity), perfluorobutanoic acid (98% purity), perfluoropropanoic acid (97% purity), nitrobenzene (≥99% purity) and fluoride standard (TraceCERT®, 1000 mg/L in water) were purchased from Millipore Sigma. Hydrogen peroxide 30% (w/v) was purchased from Fisher Scientific.

2.2. PFOA degradation using UV photolysis versus UV + H_2O_2 AOP

UVC irradiation experiments were carried out in a photoreactor that has been previously described (Lee et al., 2018; Zhang et al., 2018). Briefly, six 4W-UVC emission (254 nm) lamps (Sankyo Denki, G4T5) were used as irradiation source for PFOA degradation experiments. For UV photolytic tests, 40 mL of 1 mg/L PFOA were added to a 50 mL quartz beaker and irradiated under continuous stirring. For UV + H_2O_2 AOP tests, varying H_2O_2 concentrations (0.5, 5, 30 and 300 g/L) were amended to the PFOA solution before irradiation. The irradiation time ranged from 1 to 3 days. A wide range of H_2O_2 concentrations were used (0.5–5 g/L) to include concentrations that are typically used by researchers for UV-Fenton

and UV-H_2O_2 processes (Bali et al., 2004; Neamtu et al., 2002; Ruppert et al., 1994; Tang et al., 2012). We also used a 30 g/L H_2O_2 treatment (which may be too high for practical application) to benchmark against a previous study (Hori et al., 2004) and gain insight into potential inhibitory inner filter effects.

2.3. Optimization of H_2O_2 concentration using NB as •OH probe

A 40-mL aliquot of 100 mg/L NB containing varying concentrations of H_2O_2 (0.5 g/L, 1 g/L, 5 g/L, 10 g/L and 300 g/L) was added to a quartz beaker and irradiated for 30 min. Samples were analyzed at 10, 20 and 30 min intervals. •OH steady state concentration was calculated using the integrated form of pseudo first-order kinetics (Varanasi et al., 2018):

$$-\ln([NB]_t/[NB]_0) = k_{\bullet OH,NB}[\bullet OH]_{ss} \times t \qquad \text{(Equation 1)}$$

Where $[NB]_t$ and $[NB]_0$ are NB concentrations at time 0 s and t s, respectively; $k_{\bullet OH,NB}$ is the reaction rate constant between •OH and NB, which is 3.2×10^9 M^{-1} s^{-1} (Varanasi et al., 2018); and $[\bullet OH]_{ss}$ is the steady state •OH concentration (M), which is thus calculated from Equation (1) as the slope of negative $\ln(NB_t/NB_0)$ versus time divided by $k_{\bullet OH,NB}$ (Figure S2).

2.4. Light intensity measurements

Light intensity in the photoreactor was measured using ferric oxalate actinometry (Bolton et al., 2011). The photon flux in the reactor was 6×10^{-6} E/L.s (2.1 mJ/cm^2. s) corresponding to net irradiation power of 0.114 W. Light penetration experiments were conducted in LED-L16 photoreactor (Luzchem) equipped with six 7.2 W UVC (254 nm) lamps (G8T5,USHIO) which provided vertical illumination from the top. The UVC light intensity was measured using UVX Digital Radiometer (UVP). A 100-mL quartz beaker containing 40 mL solutions of varying H_2O_2 concentrations (0 g/L, 0.5 g/L, 5 g/L, 10 g/L and 300 g/L) was placed on the radiometer detector and irradiated. Light intensity readings were recorded after a 3-min stabilization period.

2.5. EE/O and F$^-$ calculations

The EE/O (kWh/m^3·order) was calculated as:

$$EE\Big/O = \frac{P \times \left(\frac{t}{60}\right) \times 1000}{V \times \log\left(\frac{C_0}{C}\right)} \qquad \text{(Equation 2)}$$

where P is the actinometrically determined power (kW), V is the irradiated volume (L), C and C_0 are concentrations of PFOA at time t min and 0 min, respectively.

The PFOA defluorination efficiency (%) was calculated as:

$$\text{Defluorination efficiency (\%)} = \frac{[F^-] \text{ released}}{\text{Total } [F] \text{ originally in PFOA}} \times 100$$

$$\text{(Equation 3)}$$

2.6. Analytical methods

PFOA and its degradation by-products were analyzed by high performance liquid chromatography (Agilent 1200, Agilent Technologies) using a C18 column (Ascentis Express, 2.7 μm, 15 cm × 2.1 mm) and mass detector (MicroTOF, Bruker). The mobile

phase was 60% acetonitrile with 0.1% formic acid and 40% water with 0.1% formic acid. The flow rate was 0.35 mL/min and the column was maintained at 80 °C. NB was analyzed using a HPLC (LC20AT, Shimadzu) equipped with a C-18 column (Atlantis, 3 μm, 3.9 mm × 150 mm) and an UV−Vis photodiode array detector (SPD-M20A, Shimadzu). 60% acetonitrile and 40% water were used as the mobile phase with 1 mL/min flow rate. Fluoride (F^-) was measured using an ion chromatography (IC) system (Dionex Aquion) equipped with an anion-exchange column (Dionex, RFIC™ IonPac™ AS23 column, 4 × 250 mm), and a conductivity detector (Dionex, DS6 heated conductivity cell). The mobile phase was an aqueous solution containing sodium carbonate (4.5 mM) and sodium bicarbonate (0.8 mM) at an isocratic flow rate of 1 mL/min.

All experiments were replicated, and single factor ANOVA was used to determine whether differences in results were statistically significant at the 95% confidence level.

3. Results and discussion

NB was used as a •OH probe to optimize the H_2O_2 concentration and maximize •OH production in our photoreactor (Li et al., 2017; Varanasi et al., 2018). A concentration of 5 g/L H_2O_2 resulted in the highest •OH production, removing 94 ± 0.2% of 100 mg/L NB within 30 min under UV irradiation (Fig. 1). This corresponded to a steady state •OH concentration of $4.56 \times 10^{-13} \pm 3.84 \times 10^{-15}$ M (Table S1). H_2O_2 concentrations greater than 5 g/L were counterproductive to •OH generation due to potential scavenging of both •OH and UV light (inner filter effect) by H_2O_2 (Buxton et al., 1988; Nienow et al., 2008; Xu et al., 2009). This was corroborated by light penetration experiments, which revealed that higher H_2O_2 concentrations significantly hindered light penetration across the aqueous solution (Figure S3). Subsequently, 1-day UV irradiation experiments were conducted to compare PFOA removal by UV photolysis and UV + H_2O_2 AOP at optimized H_2O_2 concentrations to evaluate the efficacy of •OH for PFOA degradation.

Under optimized H_2O_2 amendment (5 g/L), •OH did not enhance PFOA removal by UV (Fig. 2). Removal efficiencies were 19.7 ± 0.7% for optimized UV + H_2O_2 AOP versus 21.1 ± 0.4% for treatment by UV photolysis. This indicates that direct photolysis was the main PFOA degradation mechanism. Further evidence of the insignificant role of •OH was provided by by-product analysis, where the three
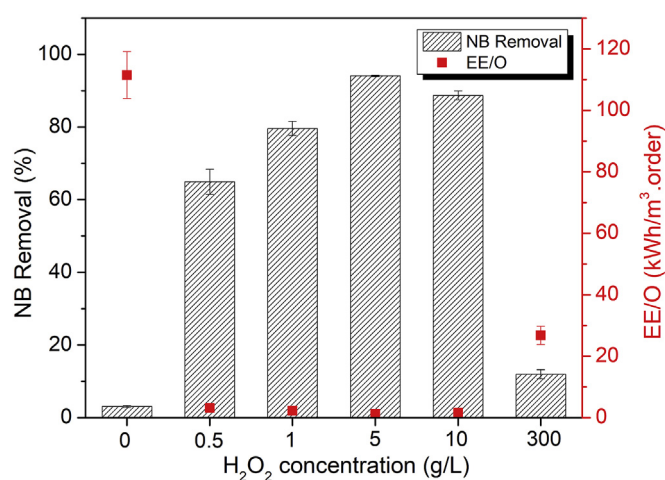
Fig. 2. PFOA (1 mg/L) degradation by UV photolysis and UV + H_2O_2 (0.5 g/L, 5 g/L or 30 g/L) AOP after 1-day UV irradiation. UV photolysis and UV + H_2O_2 (0.5 g/L, 5 g/L and 30 g/L) AOP removed 21.1 ± 0.4%, 22.6 ± 1.3%,19.7 ± 0.7% and 2.8 ± 0.4% PFOA, respectively. No statistically significant difference (F < F_{crit} and p > 0.05, ANOVA) in PFOA removal was observed between UV photolysis and UV + H_2O_2 (0.5 g/L or 5 g/L) treatments.

treatment processes (UV photolysis, and UV + H_2O_2 (0.5 or 5 g/L)) yielded identical concentrations of C4, C5, C6 and C7 daughter by-products (Table 1). In addition, no statistically significant difference (F < F_{crit} and p > 0.05) was found between the defluorination efficiencies for the three treatment processes (Table 2). The consistent extent of PFOA degradation observed at different H_2O_2 concentrations (0 g/L, 0.5 g/L and 5 g/L) corroborates that, regardless of matrix differences and effective irradiation dose, direct UV photolysis was the main PFOA degradation mechanism and that •OH played an insignificant role. Complete F^- mass balance was achieved in our treatment systems with F^- ion, shorter-chain daughter by-products, and PFOA accounting for 97%−108% of the total F^- in the system (Text S1 and Table S2).

PFOA degradation at an impractically high H_2O_2 concentration (30 g/L) was also investigated to benchmark against a previous study (Hori et al., 2004) and more easily illustrate potential inhibitory effects associated with the high molar absorptivity of H_2O_2 at 254 nm. UV + H_2O_2 (30 g/L) was counter-productive to PFOA degradation as excess H_2O_2 caused ineffective UV irradiation due to an inner filter effect that hindered UV penetration (Figure S3) and PFOA photolysis (Fig. 2 and Table 1). This illustrates a potential drawback about efforts to intensify AOPs by increasing the H_2O_2 dose.

In this study, PFOA treatment efficiencies were compared for UV

Fig. 1. Optimization of H_2O_2 concentration using NB as •OH probe. The optimum H_2O_2 concentration was about 5 g/L H_2O_2, which removed 94 ± 0.2% NB (100 mg/L) after 30 min UV irradiation (2.1 mJ/cm^2. s) with an EE/O of 1.23 ± 0.01 kWh/m^3. order. Inner-filter effect, and consumption of •OH by H_2O_2 scavenging and •OH self-recombination made concentrations greater than 5 g/L ineffective.
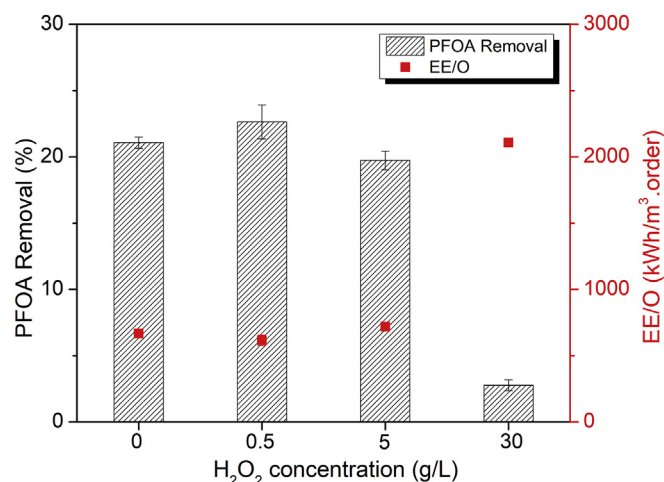
Table 1
Concentrations of PFOA degradation by-products in UV and UV + H_2O_2 (0.5 g/L, 5 g/L and 30 g/L) treatment systems after 1-day UV irradiation.

Sample	PFOA Byproduct Concentration (mg/L)				
	C3	C4	C5	C6	C7
Photolysis 1day	ND	BQL	BQL	0.023 ± 0.002	0.146 ± 0.012
UV + H_2O_2 (0.5 g/L) 1 day	ND	BQL	BQL	0.022 ± 0.002	0.156 ± 0.006
UV + H_2O_2 (5 g/L) 1 day	ND	BQL	BQL	0.022 ± 0.005	0.169 ± 0.009
UV + H_2O_2 (30 g/L) 1 day	ND	ND	ND	ND	0.012 ± 0.006

BQL = Below quantification limit (0.01 mg/L); ND = Not detected (LOD = 0.003 mg/L).

Table 2
PFOA defluorination efficiencies following treatment by UV photolysis or UV + H_2O_2 (0.5 or 5 g/L) AOP after 1-day UV irradiation.

Samples	Defluorination efficiency (%)
Photolysis 1 day	9.5 ± 1.7*
UV + H_2O_2 (0.5 g/L) 1 day	6.9 ± 0.9*
UV + H_2O_2 (5 g/L) 1 day	6.8 ± 1.0*

* No statistically significant difference (F < F_{crit} and p > 0.05, Analysis of Variance (ANOVA)).

Limit of detection (LOD) for F^- was 0.015 mg/L. Defluorination efficiencies could not be determined for higher concentrations due to interference by residual H_2O_2.

photolysis and UV + H_2O_2 AOP under constant UV exposure times (instead of constant UV dose) in order to lend practical applicability to our results and demonstrate that (under similar contact times) (1) amendment of H_2O_2 does not enhance PFOA degradation due to the inefficacy of hydroxyl radicals, and (2) high H_2O_2 concentrations can be inhibitory to PFOA degradation due to UV light scavenging by H_2O_2. Others studies have also used constant exposure times to compare treatment efficiency and generated radical concentrations in photochemical systems (Hori et al., 2004; Li et al., 2017; Liu et al., 2013; Tang et al., 2012; Varanasi et al., 2018).

Possible PFOA degradation pathways in the presence of •OH under UV irradiation are shown in Fig. 3 (Hori et al., 2004; Liu et al., 2013; Tang et al., 2012). The UV photolytic degradation of PFOA is most likely initiated by C−C scission through Photo-Kolbe decarboxylation reaction (pathway 2) (Hori et al., 2004, 2002; Huang et al., 2016a). This forms •C_7F_{15} which may be converted to shorter-chain perfluorinated carboxylic acid daughter by-product, $C_6F_{13}COOH$ (C7) via hydrolysis of an unstable perfluorinated alcohol intermediate ($C_7F_{15}OH$) (Hori et al., 2004; Liu et al., 2013; Nohara et al., 2001). Hence, PFOA is converted to C7 by loss of a CF_2 unit. Further degradation of C7 may proceed via loss of another CF_2 unit (Wang et al., 2008). This stepwise degradation of PFOA via successive losses of CF_2 units is corroborated by analysis of degradation by-products where concentrations of perfluorinated

daughter by-products also follow a successive order i.e.: [C3] < [C4] < [C5] < [C6] < [C7] (Hori et al., 2004; Wang et al., 2008). The •OH could theoretically assist the PFOA degradation by either initiating decarboxylation (pathway 1) or by accelerating the conversion of intermediate perfluorinated radical to perfluorinated alcohol (pathway 3). However, our study shows that the contribution of •OH through either of these pathways is insignificant because UV irradiation alone was as effective as when the •OH concentration was maximized in the UV + H_2O_2 treatment.

Overall, this study shows that direct photolysis of PFOA by UV irradiation is the primary degradation mechanism during treatment by UV + H_2O_2 AOP, and infers that treatment processes that consume too much of the incident UV irradiation to produce •OH (e.g., H_2O_2 amendment) are counter-productive to PFOA degradation due to hindered photolysis. Therefore, future work on PFOA degradation should explore other mechanisms independent of •OH production. Furthermore, past studies reporting enhanced PFOA degradation by •OH must be re-examined to determine whether •OH may participate indirectly in other pertinent processes, such as enhanced regeneration of Fe(III) in UV-Fenton and UV + Fe(III) systems.

Associated content

Supporting Information includes: (1) F^- mass balance calculations and further details on EE/O calculations. (2) Figures of PFOA degradation mechanism in UV-Fenton and UV-Fe(III) treatment systems, -ln(NB_t/NB_0) versus time plots for NB degradation, light penetration experiments, and PFOA degradation by UV + H_2O_2 (300 g/L) over 3-day UV exposure. (3) Tables of •OH concentrations at different H_2O_2 concentrations, and F^- mass balance.

CRediT author statement

Hassan Javed: contributed intellectual input to this study, Conceptualization, Methodology, Investigation, Writing - original draft. Cong Lyu: contributed intellectual input to this study, Methodology, Investigation. Ruonan Sun: contributed intellectual input to this study, Investigation. Danning Zhang: contributed intellectual input to this study, Investigation, Visualization. Pedro J.J. Alvarez: contributed intellectual input to this study, Conceptualization, Supervision, Funding acquisition, Writing - review & editing.

Acknowledgements

Appendix A. Supplementary data

Supplementary data related to this article can be found at https://doi.org/10.1016/j.chemosphere.2020.125883.

Fig. 3. Proposed PFOA degradation pathway in UV and UV + H_2O_2 treatment systems. The degradation mechanism is adapted from Hori et al., Liu et al. and Tang et al.(Hori et al., 2004; Liu et al., 2013; Tang et al., 2012) In UV photolytic process, PFOA degradation is initiated by C−C scission via Photo-Kolbe decarboxylation (pathway 2). In UV + H_2O_2 AOP, •OH has been proposed to enhance PFOA degradation by either initiating decarboxylation (pathway 1) or by accelerating the conversion of perfluorinated organic radical to perfluorinated alcohol (pathway 3)(Liu et al., 2013). Contribution of •OH in enhancing PFOA removal via pathways 1 and 3 was insignificant in this study.

References

Arvaniti, O.S., Hwang, Y., Andersen, H.R., Stasinakis, A.S., Thomaidis, N.S., Aloupi, M., 2015. Reductive degradation of perfluorinated compounds in water using Mg-aminoclay coated nanoscale zero valent iron. Chem. Eng. J. 262, 133−139. https://doi.org/10.1016/J.CEJ.2014.09.079.

Bali, U., Çatalkaya, E., Şengül, F., 2004. Photodegradation of reactive black 5, direct red 28 and direct yellow 12 using UV, UV/H_2O_2 and UV/H_2O_2/Fe^{2+}: a comparative study. J. Hazard Mater. 114, 159−166. https://doi.org/10.1016/J.JHAZMAT.2004.08.013.

Bolton, J.R., Stefan, M.I., Shaw, P.-S., Lykke, K.R., 2011. Determination of the quantum yields of the potassium ferrioxalate and potassium iodide−iodate actinometers and a method for the calibration of radiometer detectors. J. Photochem.
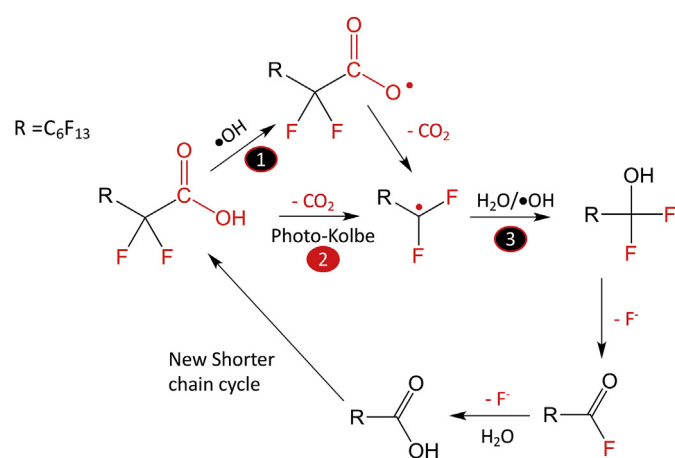
Photobiol. A Chem. 222, 166–169. https://doi.org/10.1016/J.JPHOTOCHEM.2011.05.017.

Buxton, G.V., Greenstock, C.L., Helman, W.P., Ross, A.B., 1988. Critical Review of rate constants for reactions of hydrated electrons, hydrogen atoms and hydroxyl radicals (·OH/·O− in Aqueous Solution. J. Phys. Chem. Ref. Data 17, 513–886. https://doi.org/10.1063/1.555805.

Chen, M.-J., Lo, S.-L., Lee, Y.-C., Huang, C.-C., 2015. Photocatalytic decomposition of perfluorooctanoic acid by transition-metal modified titanium dioxide. J. Hazard Mater. 288, 168–175. https://doi.org/10.1016/J.JHAZMAT.2015.02.004.

Chen, M.-J., Lo, S.-L., Lee, Y.-C., Kuo, J., Wu, C.-H., 2016. Decomposition of perfluorooctanoic acid by ultraviolet light irradiation with Pb-modified titanium dioxide. J. Hazard Mater. 303, 111–118. https://doi.org/10.1016/J.JHAZMAT.2015.10.011.

Chen, Y.-C., Lo, S.-L., Kuo, J., 2011. Effects of titanate nanotubes synthesized by a microwave hydrothermal method on photocatalytic decomposition of perfluorooctanoic acid. Water Res. 45, 4131–4140. https://doi.org/10.1016/J.WATRES.2011.05.020.

Cheng, J., Vecitis, C.D., Park, H., Mader, B.T., Hoffmann, M.R., 2008. Sonochemical degradation of perfluorooctane sulfonate (PFOS) and perfluorooctanoate (PFOA) in landfill groundwater: environmental matrix effects. Environ. Sci. Technol. 42, 8057–8063. https://doi.org/10.1021/es8013858.

Eberle, D., Ball, R., Boving, T.B., 2017. Impact of ISCO treatment on PFAA Co-contaminants at a former fire training area. Environ. Sci. Technol. 51, 5127–5136. https://doi.org/10.1021/acs.est.6b06591.

Ellis, D.A., Martin, J.W., Silva, A.O. De, Mabury, S.A., Hurley, M.D., Andersen, M.P.S., Wallington, T.J., 2004. Degradation of fluorotelomer alcohols: a likely atmospheric source of perfluorinated carboxylic acids. Environ. Sci. Technol. 38, 3316–3321. https://doi.org/10.1021/ES049860W.

Gomez-Ruiz, B., Gómez-Lavín, S., Diban, N., Boiteux, V., Colin, A., Dauchy, X., Urtiaga, A., 2017. Efficient electrochemical degradation of poly- and per-fluoroalkyl substances (PFASs) from the effluents of an industrial wastewater treatment plant. Chem. Eng. J. 322, 196–204. https://doi.org/10.1016/J.CEJ.2017.04.040.

Gomez-Ruiz, B., Ribao, P., Diban, N., Rivero, M.J., Ortiz, I., Urtiaga, A., 2018. Photocatalytic degradation and mineralization of perfluorooctanoic acid (PFOA) using a composite TiO2 −rGO catalyst. J. Hazard Mater. 344, 950–957. https://doi.org/10.1016/J.JHAZMAT.2017.11.048.

Gómez, C., Vicente, J., Echavarri-Erasun, B., Porte, C., Lacorte, S., 2011. Occurrence of perfluorinated compounds in water, sediment and mussels from the Cantabrian Sea (North Spain). Mar. Pollut. Bull. 62, 948–955. https://doi.org/10.1016/J.MARPOLBUL.2011.02.049.

Hori, H., Hayakawa, E., Einaga, H., Kutsuna, S., Koike, K., Ibusuki, T., Kiatagawa, H., Arakawa, R., 2004. Decomposition of environmentally persistent perfluorooctanoic acid in water by photochemical approaches. Environ. Sci. Technol. 38, 6118–6124. https://doi.org/10.1021/ES049719N.

Hori, H., Nagaoka, Y., Yamamoto, A., Sano, T., Yamashita, N., Taniyasu, S., Kutsuna, S., Osaka, I., Arakawa, R., 2006. Efficient decomposition of environmentally persistent perfluorooctanesulfonate and related fluorochemicals using zer-ovalent iron in subcritical water. Environ. Sci. Technol. 40, 1049–1054. https://doi.org/10.1021/ES0517419.

Hori, H., Takano, Y., Koike, K., Takeuchi, K., Einaga, H., 2002. Decomposition of environmentally persistent trifluoroacetic acid to fluoride ions by a homogeneous photocatalyst in water. Environ. Sci. Technol. 37, 418–422. https://doi.org/10.1021/ES025783Y.

Hori, H., Yamamoto, A., Hayakawa, E., Taniyasu, S., Yamashita, N., Kutsuna, S., Kiatagawa, H., Arakawa, R., 2005. Efficient decomposition of environmentally persistent perfluorocarboxylic acids by use of persulfate as a photochemical oxidant. Environ. Sci. Technol. 39, 2383–2388. https://doi.org/10.1021/ES0484754.

Huang, D., Yin, L., Niu, J., 2016a. Photoinduced hydrodefluorination mechanisms of perfluorooctanoic acid by the SiC/graphene catalyst. Environ. Sci. Technol. 50, 5857–5863. https://doi.org/10.1021/acs.est.6b00652.

Huang, J., Wang, X., Pan, Z., Li, X., Ling, Y., Li, L., 2016b. Efficient degradation of perfluorooctanoic acid (PFOA) by photocatalytic ozonation. Chem. Eng. J. 296, 329–334. https://doi.org/10.1016/J.CEJ.2016.03.116.

Ju, X., Jin, Y., Sasaki, K., Saito, N., 2008. Perfluorinated surfactants in surface, sub-surface water and microlayer from dalian coastal waters in China. Environ. Sci. Technol. 42, 3538–3542. https://doi.org/10.1021/es703006d.

Khan, S.J., Gagnon, G.A., Templeton, M.R., Dionysiou, D.D., 2018. The rapidly growing role of UV-AOPs in the production of safe drinking water. Environ. Sci. Water Res. Technol. 4, 1211–1212. https://doi.org/10.1039/C8EW90033G.

Le, T.X.H., Haflich, H., Shah, A.D., Chaplin, B.P., 2019. Energy-efficient electrochemical oxidation of perfluoroalkyl substances using a Ti 4 O 7 reactive electrochemical membrane anode. Environ. Sci. Technol. Lett. 6, 504–510. https://doi.org/10.1021/acs.estlett.9b00397.

Lee, C.-G., Javed, H., Zhang, D., Kim, J.-H., Westerhoff, P., Li, Q., Alvarez, P.J.J., 2018. Porous electrospun fibers embedding TiO2 for adsorption and photocatalytic degradation of water pollutants. Environ. Sci. Technol. 52, 4285–4293. https://doi.org/10.1021/acs.est.7b06508.

Li, W., Jain, T., Ishida, K., Liu, H., 2017. A mechanistic understanding of the degradation of trace organic contaminants by UV/hydrogen peroxide, UV/persulfate and UV/free chlorine for water reuse. Environ. Sci. Water Res. Technol. 3, 128–138. https://doi.org/10.1039/C6EW00242K.

Lin, H., Niu, J., Ding, S., Zhang, L., 2012. Electrochemical degradation of perfluorooctanoic acid (PFOA) by Ti/SnO2−Sb, Ti/SnO2−Sb/PbO2 and Ti/SnO2−Sb/

MnO2 anodes. Water Res. 46, 2281–2289. https://doi.org/10.1016/J.WATRES.2012.01.053.

Lin, J.-C., Lo, S.-L., Hu, C.-Y., Lee, Y.-C., Kuo, J., 2015. Enhanced sonochemical degradation of perfluorooctanoic acid by sulfate ions. Ultrason. Sonochem. 22, 542–547. https://doi.org/10.1016/J.ULTSONCH.2014.06.006.

Liou, J.S.C., Szostek, B., DeRito, C.M., Madsen, E.L., 2010. Investigating the biodegradability of perfluorooctanoic acid. Chemosphere 80, 176–183. https://doi.org/10.1016/j.chemosphere.2010.03.009.

Liu, C.S., Higgins, C.P., Wang, F., Shih, K., 2012. Effect of temperature on oxidative transformation of perfluorooctanoic acid (PFOA) by persulfate activation in water. Separ. Purif. Technol. 91, 46–51. https://doi.org/10.1016/J.SEPPUR.2011.09.047.

Liu, D., Xiu, Z., Liu, F., Wu, G., Adamson, D., Newell, C., Vikesland, P., Tsai, A.-L., Alvarez, P.J., 2013. Perfluorooctanoic acid degradation in the presence of Fe(III) under natural sunlight. J. Hazard Mater. 262, 456–463. https://doi.org/10.1016/J.JHAZMAT.2013.09.001.

Lopes da Silva, F., Laitinen, T., Pirilä, M., Keiski, R.L., Ojala, S., 2017. Photocatalytic degradation of perfluorooctanoic acid (PFOA) from wastewaters by TiO2, In2O3 and Ga2O3 catalysts. Top. Catal. 60, 1345–1358. https://doi.org/10.1007/s11244-017-0819-8.

Mitchell, S.M., Ahmad, M., Teel, A.L., Watts, R.J., 2014. Degradation of perfluorooctanoic acid by reactive species generated through catalyzed H2O2 propagation reactions. Environ. Sci. Technol. Lett. 1, 117–121. https://doi.org/10.1021/ez4000862.

Neamtu, M., Siminiceanu, I., Yediler, A., Kettrup, A., 2002. Kinetics of decolorization and mineralization of reactive azo dyes in aqueous solution by the UV/H2O2 oxidation. Dyes Pigments 53, 93–99. https://doi.org/10.1016/S0143-7208(02)00012-8.

Nienow, A.M., Bezares-Cruz, J.C., Poyer, I.C., Hua, I., Jafvert, C.T., 2008. Hydrogen peroxide-assisted UV photodegradation of Lindane. Chemosphere 72, 1700–1705. https://doi.org/10.1016/J.CHEMOSPHERE.2008.04.080.

Nohara, K., Toma, M., Kutsuna, S., Takeuchi, Koji, Ibusuki, T., 2001. Cl atom-initiated oxidation of three homologous methyl perfluoroalkyl ethers. Environ. Sci. Technol. 35, 114–120. https://doi.org/10.1021/ES000895F.

Park, H., Vecitis, C.D., Cheng, J., Choi, W., Mader, B.T., Hoffmann, M.R., 2009. Reductive defluorination of aqueous perfluorinated alkyl surfactants: effects of ionic headgroup and chain length. J. Phys. Chem. A 113, 690–696. https://doi.org/10.1021/jp807116q.

Ruppert, G., Bauer, R., Heisler, G., 1994. UV-O3, UV-H2O2, UV-TiO2 and the photo-Fenton reaction - comparison of advanced oxidation processes for wastewater treatment. Chemosphere 28, 1447–1454. https://doi.org/10.1016/0045-6535(94)90239-9.

Saleh, N.B., Khalid, A., Tian, Y., Ayres, C., Sabaraya, I.V., Pietari, J., Hanigan, D., Chowdhury, I., Apul, O.G., 2019. Removal of poly- and per-fluoroalkyl substances from aqueous systems by nano-enabled water treatment strategies. Environ. Sci. Water Res. Technol. 5, 198–208. https://doi.org/10.1039/C8EW00621K.

Schaefer, C.E., Andaya, C., Burant, A., Condee, C.W., Urtiaga, A., Strathmann, T.J., Higgins, C.P., 2017. Electrochemical treatment of perfluorooctanoic acid and perfluorooctane sulfonate: insights into mechanisms and application to groundwater treatment. Chem. Eng. J. 317, 424–432. https://doi.org/10.1016/J.CEJ.2017.02.107.

Song, C., Chen, P., Wang, C., Zhu, L., 2012. Photodegradation of perfluorooctanoic acid by synthesized TiO2–MWCNT composites under 365 nm UV irradiation. Chemosphere 86, 853–859. https://doi.org/10.1016/J.CHEMOSPHERE.2011.11.034.

Song, Z., Tang, H., Wang, N., Zhu, L., 2013. Reductive defluorination of perfluorooctanoic acid by hydrated electrons in a sulfite-mediated UV photochemical system. J. Hazard Mater. 262, 332–338. https://doi.org/10.1016/J.JHAZMAT.2013.08.059.

Suja, F., Pramanik, B.K., Zain, S.M., 2009. Contamination, bioaccumulation and toxic effects of perfluorinated chemicals (PFCs) in the water environment: a review paper. Water Sci. Technol. 60, 1533–1544. https://doi.org/10.2166/wst.2009.504.

Szajdzinska-Pietek, E., Gebicki, J.L., 2000. Pulse radiolytic investigation of perfluorinated surfactants in aqueous solutions. Res. Chem. Intermed. 26, 897–912. https://doi.org/10.1163/156856700X00381.

Tang, H., Xiang, Q., Lei, M., Yan, J., Zhu, L., Zou, J., 2012. Efficient degradation of perfluorooctanoic acid by UV–Fenton process. Chem. Eng. J. 184, 156–162. https://doi.org/10.1016/J.CEJ.2012.01.020.

Urtiaga, A., Fernández-González, C., Gómez-Lavín, S., Ortiz, I., 2015. Kinetics of the electrochemical mineralization of perfluorooctanoic acid on ultrananocrystalline boron doped conductive diamond electrodes. Chemosphere 129, 20–26. https://doi.org/10.1016/J.CHEMOSPHERE.2014.05.090.

Varanasi, L., Coscarelli, E., Khaksari, M., Mazzoleni, L.R., Minakata, D., 2018. Transformations of dissolved organic matter induced by UV photolysis, Hydroxyl radicals, chlorine radicals, and sulfate radicals in aqueous-phase UV-Based advanced oxidation processes. Water Res. 135, 22–30. https://doi.org/10.1016/J.WATRES.2018.02.015.

Vecitis, C.D., Park, H., Cheng, J., Mader, B.T., Hoffmann, M.R., 2008. Kinetics and mechanism of the sonolytic conversion of the aqueous perfluorinated surfactants, perfluorooctanoate (PFOA), and perfluorooctane sulfonate (PFOS) into inorganic products. J. Phys. Chem. 112, 4261–4270. https://doi.org/10.1021/JP801081Y.

Vestergren, R., Cousins, I.T., Trudel, D., Wormuth, M., Scheringer, M., 2008.

Estimating the contribution of precursor compounds in consumer exposure to PFOS and PFOA. Chemosphere 73, 1617–1624. https://doi.org/10.1016/J.CHEMOSPHERE.2008.08.011.

Wang, Y., Zhang, P., Pan, G., Chen, H., 2008. Ferric ion mediated photochemical decomposition of perfluorooctanoic acid (PFOA) by 254 nm UV light. J. Hazard Mater. 160, 181–186. https://doi.org/10.1016/J.JHAZMAT.2008.02.105.

Xu, B., Gao, N., Cheng, H., Xia, S., Rui, M., Zhao, D., 2009. Oxidative degradation of dimethyl phthalate (DMP) by UV/H2O2 process. J. Hazard Mater. 162, 954–959. https://doi.org/10.1016/J.JHAZMAT.2008.05.122.

Zhang, D., Lee, C., Javed, H., Yu, P., Kim, J.-H., Alvarez, P.J.J., 2018. Easily recoverable, micrometer-sized TiO$_2$ hierarchical spheres decorated with cyclodextrin for enhanced photocatalytic degradation of organic micropollutants. Environ. Sci. Technol. 52, 12402–12411. https://doi.org/10.1021/acs.est.8b04301.

Zhang, Y., Moores, A., Liu, J., Ghoshal, S., 2019. New insights into the degradation mechanism of perfluorooctanoic acid by persulfate from density functional theory and experimental data. Environ. Sci. Technol. 53, 8672–8681. https://doi.org/10.1021/acs.est.9b00797.

Zhuo, Q., Deng, S., Yang, B., Huang, J., Yu, G., 2011. Efficient electrochemical oxidation of perfluorooctanoate using a Ti/SnO$_2$-Sb-Bi anode. Environ. Sci. Technol. 45, 2973–2979. https://doi.org/10.1021/es1024542.